Spine Deformity (2020) 8:853–862
https://doi.org/10.1007/s43390-020-00108-2

BIOMECHANICS

Biomechanical comparison of sacral and transarticular sacroiliac screw fixation

Léo Fradet[1,2,3] · Rohan-Jean Bianco[1,4,5] · Robert Tatsumi[6] · John Coleman[7] · Carl-Éric Aubin[1,2,3]

Received: 4 March 2020 / Accepted: 16 March 2020 / Published online: 9 April 2020

Abstract

Study design A detailed finite element analysis of screw fixation in the sacrum and pelvis.

Objective To biomechanically assess and compare the fixation performance of sacral and transarticular sacroiliac screws.

Summary of background data Instrumentation constructs are used to achieve fixation and stabilization for the treatment of spinopelvic pathologies. The optimal screw trajectory and type of bone engagement to caudally anchor long fusion constructs are not yet known.

Methods A detailed finite element model of the sacroiliac articulation with two different bone densities was developed. Two sacral and one transarticular sacroiliac screw trajectories were modeled with different diameters (5.5 and 6.5 mm) and lengths (uni-cortical, bi-cortical and quad-cortical purchase). Axial pullout and flexion/extension toggle forces were applied on the screws representing intra and post-operative loads. The force–displacement results and von Mises stresses were used to characterize the failure pattern.

Results Overall, sacroiliac screws provided forces to failure 2.75 times higher than sacral fixation screws. On the contrary, the initial stiffness was approximately half as much for sacroiliac screws. High stresses were located at screw tips for the sacral trajectories and near the cortical bone screw entry points for the sacroiliac trajectory. Overall, the diameter and length of the screws had significant effects on the screw fixation (33% increase in force to failure; 5% increase in initial stiffness). A 20% drop in bone mineral density (lower bone quality) decreased the initial stiffness by 25% and the force to failure by 5–10%. High stresses and failure occurred at the screw tip for uni- and tri-cortical screws and were close to trabecular–cortical bone interface for bi-cortical and quad-cortical screws.

Conclusions Sacroiliac fixation provided better anchorage than sacral fixation. The transarticular purchase of the sacroiliac trajectory resulted in differences in failure pattern and fixation performance.

Keywords Spinopelvic instrumentation · Sacral screws · Sacroiliac screws · Finite element analysis

Introduction

Bone screws are used for the treatment of spinopelvic pathologies to achieve fixation and stabilization. Spinal surgeons have numerous options to caudally anchor long fusion constructs via screw fixation in the sacrum and pelvis. Sacroiliac screw anchoring strength is a key factor for the success of the instrumentation fixation [1]. Due to the unfavorable biomechanics of a long lever arm at the sacroiliac level, bone screws are subject to a combination of high

✉ Carl-Éric Aubin
carl-eric.aubin@polymtl.ca

1 Department of Mechanical Engineering, Polytechnique Montréal, P.O. Box 6079, Downtown Station, Montreal, QC H3C 3A7, Canada

2 Sainte-Justine University Hospital Center, 3175, Cote Sainte-Catherine Road, Montreal, QC H3T 1C5, Canada

3 International Laboratory - Spine Imaging and Biomechanics, Montreal, Canada

4 Laboratoire de Biomécanique Appliquée, UMRT24 IFSTTAR/Aix-Marseille Université, Boulevard Pierre Dramard, 13916 Marseille Cedex 20, France

5 International Laboratory - Spine Imaging and Biomechanics, Marseille, France

6 Department of Orthopaedics and Rehabilitation, Oregon Health & Sciences University, 3181, Portland, OR, USA

7 Medtronic Spine, Memphis, TN, USA

bending, shear, and pullout loads. Consequently, spinopelvic arthrodesis with screw fixation is associated with risks of mechanical complication and pseudarthrosis [2]. In particular, iliac screw insertion is a highly invasive procedure and can cause instrumentation-related pain and prominence of the instrumentation [3]. The S1-alar iliac (S1AI) screw has been described in the literature as an alternative to sacral or iliac screw [4].

The quality of screw purchase in the sacrum remains a clinical challenge because of the variability of its bone quality [2, 5, 6] and the complexity of its anatomy. The bone quality of the patient as well as the orientation of the applied load on the screw introduced two important biomechanical variables. Biomechanical [7] and clinical [8–10] studies have widely shown that S2AI screws offer less prominence and risk of revision surgery compared to iliac screws. However, biomechanical assessment of sacroiliac screws anchorage and comparison with sacral screws remain to be achieved.

For a given screw design, surgical choices include the possibility of utilizing different screw trajectories. The corresponding screws vary in diameter and length, allowing for various bone engagements ranging from uni-cortical sacral trajectories to quad-cortical sacroiliac trajectories. Thus, it may still be difficult to determine the optimal caudal anchorage strategy for a long fusion surgery.

This study investigated the screw fixation biomechanics for several sacroiliac instrumentation configurations. Such computational simulations allow the study of different types of bone purchase and screw trajectories in an environment devoid of experimental variability.

Materials and methods

The finite element model used in this study was adapted from the Spine Model for Safety and Surgery (SM2S), which was previously used in trauma and medical device biomechanical studies similar to the present context of use and validated through comparison with published experimental data [11, 12]. The pelvis was reconstructed in 3D using a series of cross-section images of the pelvis of a 50th percentile human volunteer (32-year-old Caucasian male, 75 kg, 1.75 m, with no known spinopelvic pathology) [13]. The pelvic bony structures were modeled as trabecular cores enveloped by the cortical external layer with region-specific thickness taken and adapted from the literature [13, 14]. The cortical layer of the iliac bones had regional thicknesses ranging from 0.3 to 5 mm and the sacral cortex was 1 mm thick (Fig. 1). Trabecular and cortical bones were meshed using four node tetrahedral elements of 0.4 mm characteristic length near the contact zone with the screw shaft and where there were significant topologic and geometric changes (sharp change of local surface orientation, small radius of curvature, etc.). Greater characteristic lengths

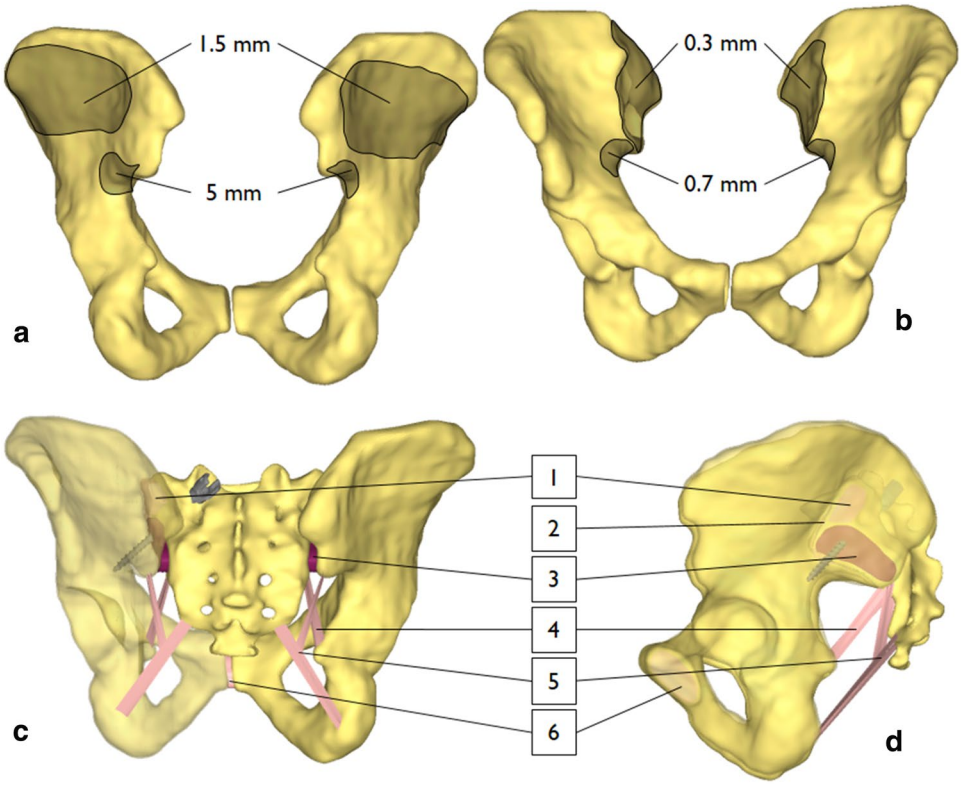

Fig. 1 Posterior (**a**) and anterior (**b**) view of the ilia with areas of different cortical thicknesses and posterior (**c**) and left (**d**) view of the instrumented sacroiliac joint including the interosseous ligament (1), anterior sacroiliac ligament (2), cartilage (3), sacrospinous ligament (4), sacrotuberous ligament (5) and pubic symphysis (6)

(around 1 mm) were used elsewhere to reduce the computational load. The screw external surface was modeled as a two-dimensional (2D) shell meshed with characteristic triangular elements of 0.4 mm. The triangle-based elements were chosen for their ability to comply with complex geometry and their non-warpage properties. The final mesh density and distribution was confirmed by a convergence study. The trabecular core and the cortical external layer were bonded through sharing common nodes along their contact surface. The screw was considered as rigid body, as its Young's modulus is far higher than those of the cortical and cancellous bones. The sacroiliac junction was modeled as a bicondylar joint in close-packed position with realistic physiologic motion [15, 16]. The pubic symphysis was represented as a single cartilaginous solid. The major pelvic ligaments (interosseous, sacroiliac anterior, sacroiliac posterior, sacrotuberous and sacrospinous) and pubic symphysis geometries were directly implemented from anatomic descriptions [17, 18]. The same method was used to create a control model of the L5 vertebra.

A Johnson–Cook elastoplastic material law was employed to simulate the bone behavior and failure [13]. The material law parameters have been calibrated for low-speed dynamics combined with kinematic relaxation (quasi-static). Once the failure plastic strain was reached on any element, it was removed to simulate its failure. The bone was considered as homogeneous isotropic material and its properties were estimated using an inverse finite element modeling (FEM) and simulation technique [19–21]. Numerical values of the mechanical material properties of the cortical and cancellous bones are provided in Table 1.

Bone mineral density (BMD) inter-individual variability was studied by defining two sets of mechanical properties (Table 1). The first set represented a normal (asymptomatic) BMD and corresponded to the nominal mechanical properties of the previously validated model. The second set represented a low (osteoporotic) BMD, which was 20% lower compared to normal bone [22]. Results reported by Keller [23] were used to define mechanical properties for the trabecular bone (20% drop in ρ corresponding to 35% drop in E). Results reported in the literature [24–26] were used for the cortical bone (20% drop in ρ corresponding to 40% drop in E).

Six screw trajectories were tested using the comprehensive FEM, namely the traditional S1 (TS1), the S1 alar (S1A), the S1 alar iliac (S1AI), the S2 alar iliac (S2AI), the L5 cortical (L5C) and the L5 traditional (L5T) trajectory (Table 2, Fig. 2). In addition to two sacral and two sacroiliac

Table 1 Mechanical properties of the cortical and cancellous bone materials

Bone quality	Cortical bone		Cancellous bone	
	Asymptomatic	Osteoporotic	Asymptomatic	Osteoporotic
Density (g/mm^3)	2.00E−03	2.00E−04	1.60E−03	1.60E−04
Young modulus (MPa)	2144	1575	42.8	31.7
Poisson ratio	0.3	0.25	0.3	0.25
Yield stress (MPa)	129	105	2.6	1.95
Hardening modulus (MPa)	875	875	16.3	16,3
Hardening exponent	1	1	1	1
Failure plastic strain	0.04	0.04	0.04	0.04

Table 2 Screw diameters and lengths (mm) used for each tested trajectory

Screw trajectory	Uni-cortical fixation	Bi-cortical fixation	Tri-cortical fixation	Quad-cortical fixation
Traditional S1 trajectory (*TS1*)	5.5×35	5.5×45		
	6.5×35	6.5 × 45		
S1-alar trajectory (*S1A*)	5.5 × 35	5.5 × 50		
	6.5 × 35	6.5 × 50		
S1-alar iliac trajectory (*S1AI*)			5.5 × 80	5.5 × 125
			6.5 × 80	6.5 × 125
S2-alar iliac trajectory (*S2AI*)			5.5 × 80	5.5 × 125
			6.5 × 80	6.5 × 125
Cortical screw trajectory in L5 (*L5C*)	5.5 × 35	5.5 × 40		
	6.5 × 35	6.5 × 40		
Traditional screw trajectory in L5 (*L5T*)	5.5 × 45	5.5 × 55		
	6.5 × 45	6.5 × 55		

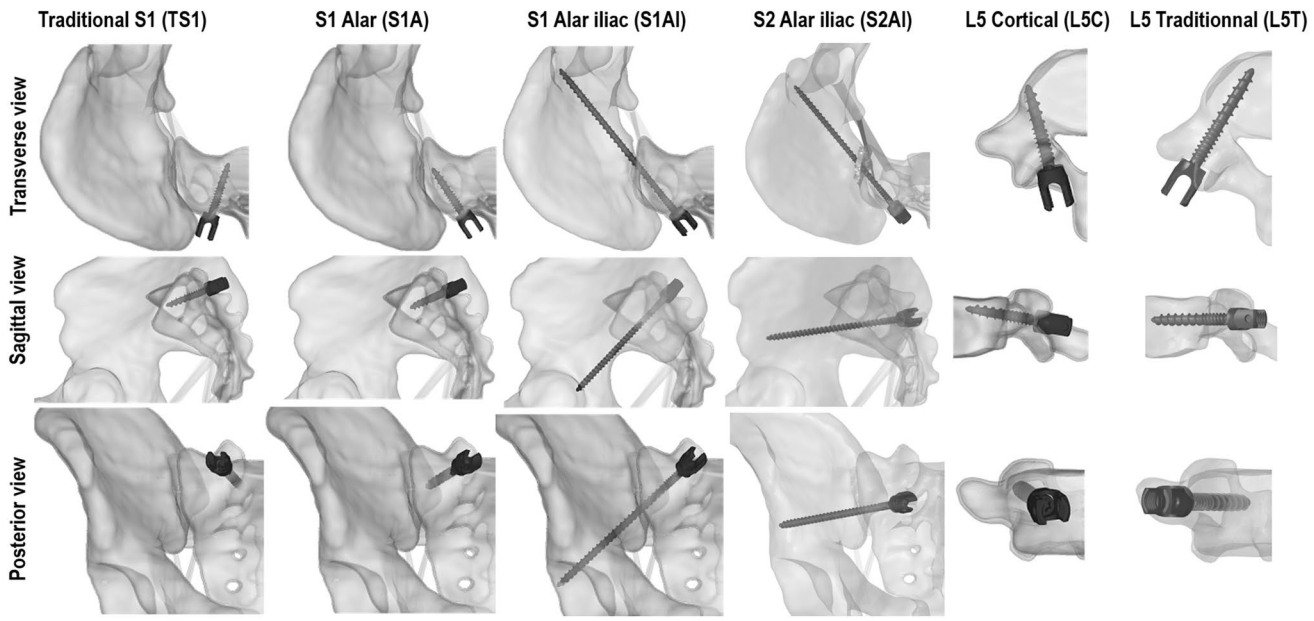

Fig. 2 Transverse and sagittal views of the four tested configurations

trajectories, a standard and a traditional L5 pedicle screw trajectory were tested and compared to references [27–32] for model validation. For each trajectory, two screw diameters were tested, as well as two screw lengths to compare uni- and bi-cortical for sacral trajectories, and tri- and quad-cortical fixations for sacroiliac trajectories, resulting in a total of 16 configurations. Two values for a given parameter were necessary to evaluate its relative influence with respect to the other tested parameters (relative vs. absolute quantification). Using 5.5 and 6.5 mm diameter screws also allowed comparison to the L5 vertebra control model for which we had experimental data, for validation purposes.

The screw insertion technique was based on previously published work [11, 12] and is summarized thereafter. The screw was placed following its assigned trajectory (Fig. 2). Bony material overlapping the screw was removed (Boolean operation) to create surfaces needed for bone–screw interface. The bone–screw interface was modeled using a point/surface penalty method with Coulomb type friction of 0.2 and minimal gap of 0.05 mm [11, 33]. Additional cortical and trabecular bone have been removed to allow for the screw head and rod to move freely when loaded.

To simulate the experimental potting conditions [34, 35], the distal third of the bone structures (sacrum for trajectories TS1 and S1A, ilium for trajectories S1AI and S2AI) was considered as a rigid body and fixed with respect to the global coordinates. For the control trajectories, the anterior third of the vertebral body was considered as a rigid body and fixed.

Pullout conditions were applied to simulate the experimental setup of the ASTM standard pullout test [36]. Accordingly, a ramped axial pullout force was applied to the screw head until complete screw pullout. The screw axial displacement and bone-implant reaction force were recorded for later analysis. Two different toggle conditions were also tested. A posterior or anterior force was applied to a rod attached to the screw, 40 mm proximal to the screw heads and parallel with the screw long axis to simulate an extension or a flexion, respectively. A ramped force was applied on the rod until complete screw pullout. Displacement and bone-implant reaction forces and moments were recorded at the proximal end of the rod for analysis.

For all loading conditions, the computed force–displacement (F–D) curves were used to determine the initial stiffness (IS, linear slope of the F–D curve) and force to failure (FtF) (Fig. 3). The IS expresses the rigidity or the ability to resist deformation in response to an applied force on the screw, whereas the FtF is the maximal force the screw can bear before bone failure.

Results

For axial pullout and toggle loading, the computed force–displacement (F–D) curves typically exhibited a non-linear behavior characterized by a neutral zone followed by a linear portion. Generalized bone failure occurred after this linear portion, characterized by a sudden drop of rigidity following which the force decreased until complete bone rupture and screw pull-out.

For both sacral trajectories (TS1, S1A), the bi-cortical 6.5 screw provided the best purchase. IS and FtF were both

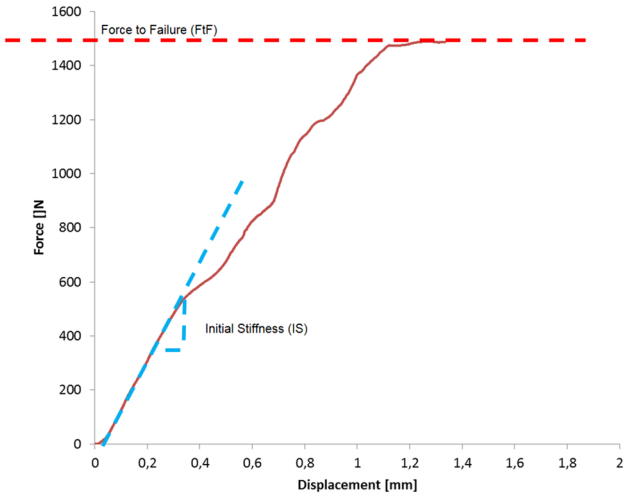

Fig. 3 Generic pullout force–displacement curve showing initial stiffness and force to failure measurement method

higher with bi-cortical insertion compared to uni-cortical and with the larger screw diameter (Figs. 4, 5). Sacroiliac trajectories provided the strongest purchase (highest FtF) in axial pullout and toggle (Fig. 4). However, the IS was the lowest for the sacroiliac trajectories. S1AI trajectory generally resulted in higher IS and FtF in pull-out compared to S2AI trajectory. Results for both sacroiliac trajectories were similar under toggle loading. For the toggle in flexion, no difference appeared between trajectories TS1, S1A, L5C and L5T, whereas for toggle in extension, the control trajectory provided the worst purchase. Under all loading conditions, a larger screw diameter and increased cortical purchase resulted in increased IS and FtF. The trajectory that benefited the most from the use of a bi-cortical insertion was the S1A trajectory, with an increase of FtF by a factor of 2 to 3. Simulations with lower mechanical properties (osteoporotic bone), resulted in a drop of 20–35% of the IS and of 5–20% of the FtF under pull-out loading, and in a drop of 5–30% in IS and of 0–25% in the FtF under toggle loading.

Fracture patterns in simulated trajectories TS1 and S1A were similar for all loading directions. Fracture initiation occurred at the screw tip in axial loading and in the trabecular bone, above (in extension) or below (in flexion) the screw (Fig. 6). Bi- and quad-cortical screws resulted in lower maximum bone stress compared to uni- and tricortical screws. For the sacroiliac trajectories, the fracture always occurred in two steps. Fracture initiation occurred in the ilium, subjecting the sacrum to higher force until final failure (Fig. 7).

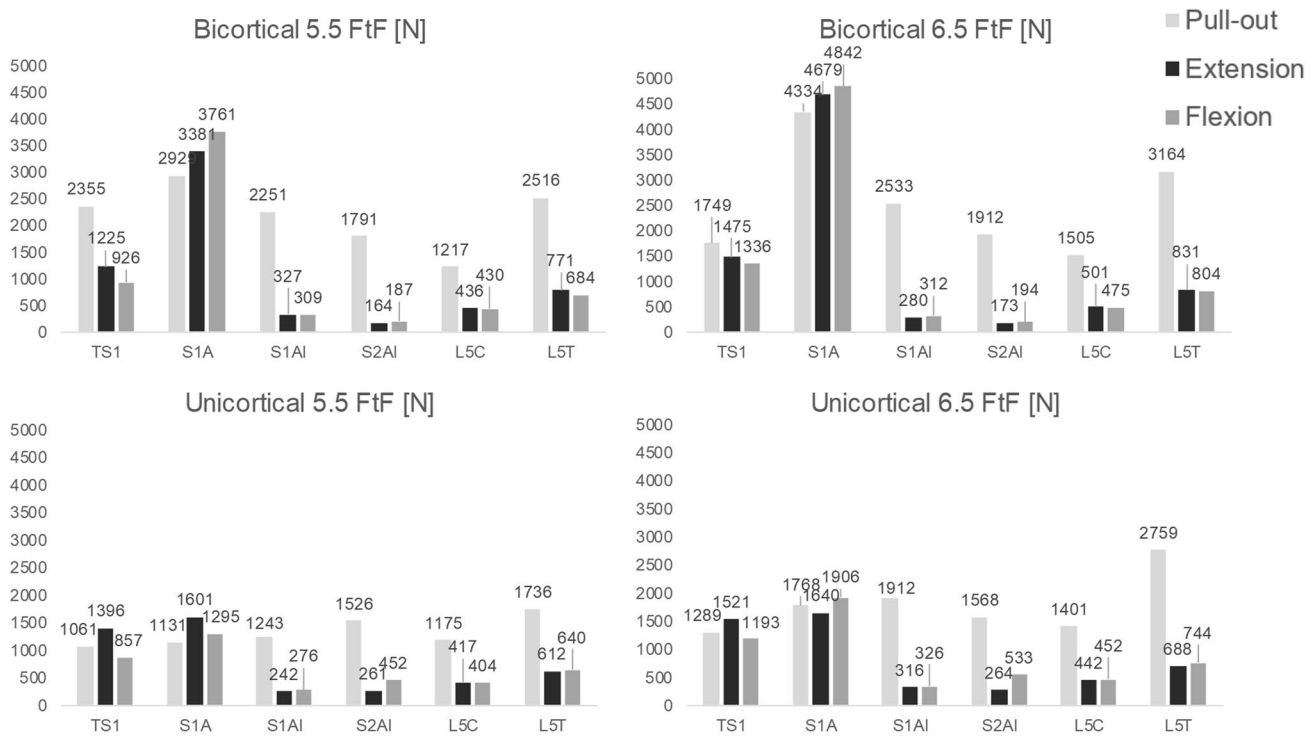

Fig. 4 Mean simulated force to failure for the 2 reference and 4 simulated sacral and sacroiliac screw insertion trajectories, with uni- or bi-cortical purchase, and 2 screw diameters, under pull-out and toggle (Flexion/extension) loading conditions

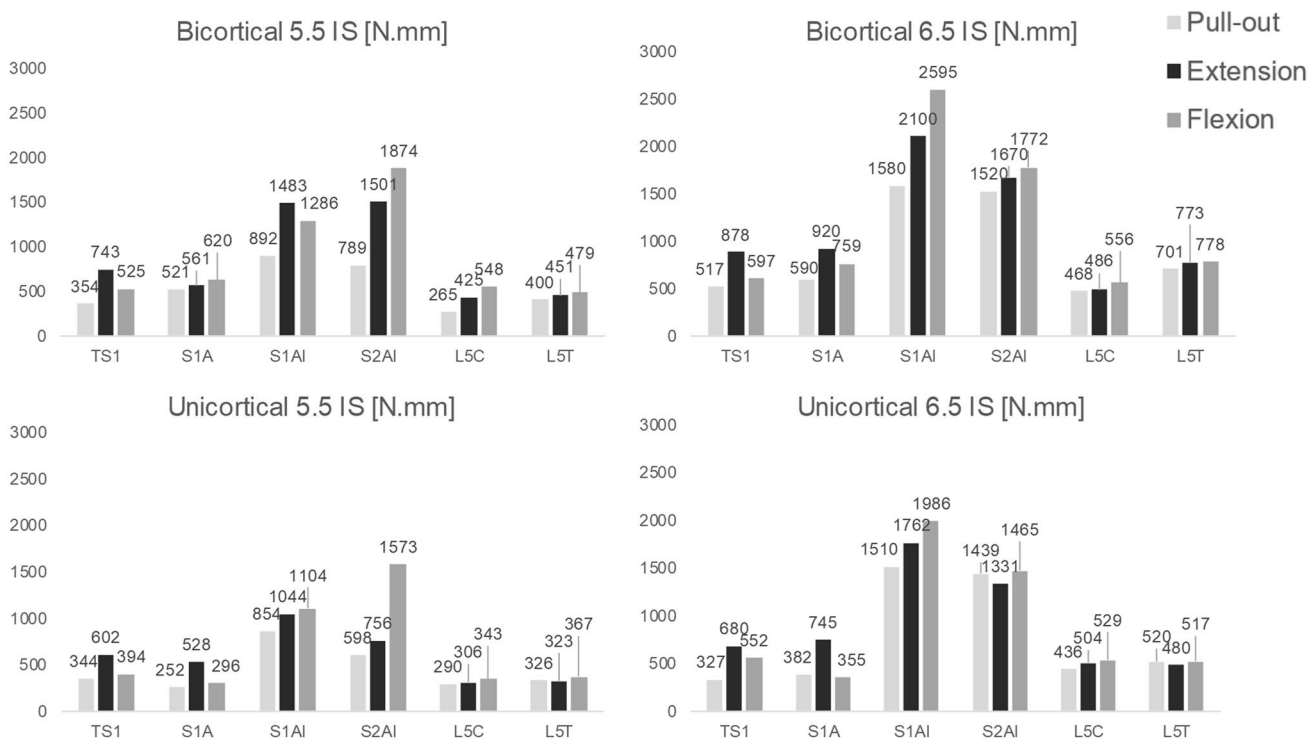

Fig. 5 Mean simulated initial stress for the 2 reference and 4 simulated sacral and sacroiliac screw insertion trajectories, with uni- or bi-cortical purchase, and 2 screw diameters, under pull-out and toggle (Flexion/extension) loading conditions

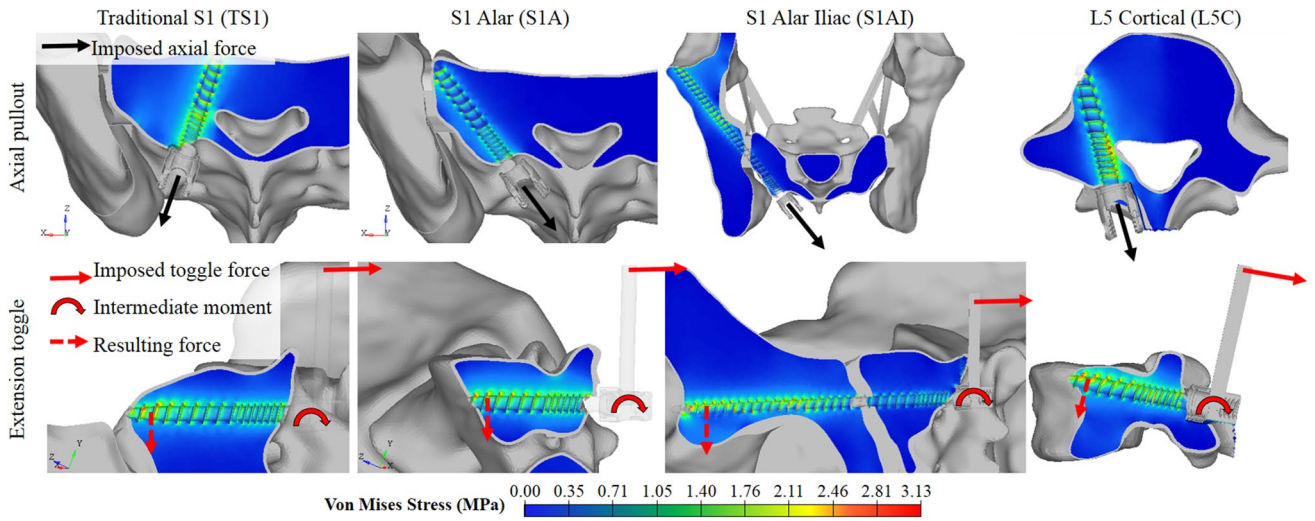

Fig. 6 Stress field in the trabecular bone resulting from cantilever effect in extension toggle. Top row shows the pullout conditions and bottom row shows the extension toggle conditions for S1AI, TS1, S1A and L5C trajectories. Arrows indicate applied and resulting forces on the screw-rod construct. S2AI and L5T trajectories were not pictured here as they were similar to S1AI and L5C, respectively

Discussion

In this study, the biomechanics of several sacral and sacroiliac screw insertion trajectories were compared under pull-out and toggle loading conditions, by analyzing the corresponding IS, FtF and the failure pattern. The use of a numerical comparative approach allowed eliminating unwanted variability of physical testing to better elucidate the isolated biomechanical effects of the studied

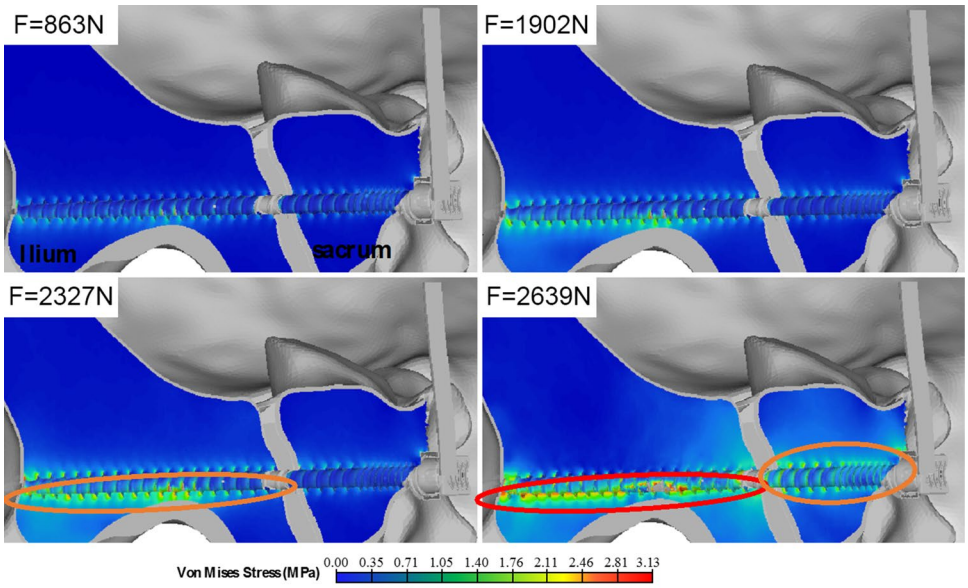

Fig. 7 Stress and fracture initiation of the trabecular bone for the S1AI with increasing flexion toggle force (F). Orange and red circles indicate high stresses and bone rupture, respectively. The fracture starts in the ilium, after which the sacrum withstands the load through the ligaments until fracture

parameters. Overall, the largest diameter (6.5 mm) screws and the more cortical bone layers traversed by the screw provided the best purchase, as reported in [11]. The biomechanics of sacroiliac trajectories were more complex, due to several factors. First, the screw crosses the interosseous ligament and sacroiliac (SI) joint. Consequently, the synergistic contribution of the two bones to sustain the load explains the smallest initial stiffness due to the SI joint mobility, compared to sacrum only insertion. Second, the sacroiliac screws are longer and penetrate three or four layers of cortical bone, as opposed to one or two for the trajectories TS1 and S1A. Thus, the highest FtF could be explained by the additional stiffer bone layers traversed by the screw along its trajectory. Although the quad-cortical purchase resulted in higher anchorage strength compared to tri-cortical insertion, this difference was shown to be non-significant in the literature [7]. Further analyses of the sacroiliac trajectories showed that most of the load was initially transferred to the ilium trabecular bone, which initially shows the highest von Mises stress. After failure of the ilium bone–screw interface, the sacrum and ligaments withstand the load, resulting in an overall nonlinear force–displacement curve. Overall, the better anchorage performance of sacroiliac trajectories and the clinical advantages of potential fewer wound complications of these trajectories [4, 7–10] suggest that it can provide a strong anchorage for long spine fusion surgical procedures. Even though the insertion point and trajectory determination might be more challenging compared to traditional sacral or lumbar insertion, this could be easily overcome by using fluoroscopic guidance [37]. S1AI and S2AI trajectories resulted in comparable anchorage performance. However, the S1A1 trajectory is a new way to provide fixation across the sacroiliac joint and offers some benefits over the more widely used S2A1 technique, as it requires less tissue disruption, smaller incision size, and less risk of injury to the sacral nerve roots. When considering strictly sacral trajectories, the TS1 trajectory, which is the standard of care in most spine surgery, was comparable or inferior to S1A trajectory, which is a newer technique.

For all simulations, the fracture initiated at the tip of the screw. Bi-cortical and quad-cortical screws allowed a better stress distribution along the screw's length in the trabecular bone. The stress analysis of control trajectory simulations showed areas of highest stress concentration around the screw close to cortical bone, which are caused by the local mechanical property gradient. In toggle, the surface of the screw head in contact with the cortical bone acted as a cantilever buttress (Fig. 6), which resulted in more displacement of the screw tip. The cantilever effect explains stress concentrations at screw tip, proximally for extension toggle loading, and distally for flexion toggle loading.

As in any numerical study, the results may have been affected by the different modeling simplifications. One of the simplifications was the use of the elastoplastic material law to represent the cancellous and cortical bones, assuming continuum and homogeneous material distribution, and isotropic mechanical properties. In reality, the sacrum and pelvis have a complex microstructure and irregular distribution with prominent anisotropic properties [14, 38, 39]; although it has been shown that discreet and continuum bone material models predict different mechanical performances (IS and FtF), so they tend to produce generally similar stress distributions [40]. Therefore, such a simplification in this project can be considered as having limited impact on the

conclusions. Another limitation was the simplification of the implant insertion process (i.e., modeling the implant recess as a Boolean subtraction of the device geometry from the bone). With this approach, the effects of drilling, tapping and the bone compaction were not considered. The bone–screw interface was idealized as contact surfaces and did not represent the damages (cracks, micro-fractures), which might be provoked during surgical screw insertion. Including such effects in a further refined model of the bone–screw interface might yield more realistic transient results and provide a better description of the local phenomena that could influence the quality of sacroiliac screw fixation. It has been demonstrated that the holding strength of a bone screw is correlated to the pilot hole geometry and preparation process, e.g. tapped or untapped [41, 42]. Screws inserted in pilot holes prepared with a 3.4-mm blunt probe (ganglion knife) resulted in higher pullout forces in eight of ten trials as compared with those with pilot holes prepared using a 3.2-mm drill. In the current study, the simulated hole preparation procedure was consistently applied across all scenarios, thus eliminating that factor while allowing comparative assessment of the specific effects of the tested trajectories and screw configurations.

A previously developed model was used as the basis for the development of the current model because it demonstrated credibility in predicting the behavior of the bone–screw interface for the context of use of investigating relative screw fixation performance, compared to earlier studies [11]. In the current work, the simulated IS (988–1720 N/mm) and FtF (241–492 N) results for the screws inserted in the control L5 vertebra were within the published range obtained experimentally on human cadaveric lumbar vertebrae (1100–2700 N/mm [27, 30] and 218–840 N [31, 32], respectively). Likewise, the lower bone density (vs. normal bone density) led to a decrease of the IS (− 20% to − 35%) and FtF (− 5% to − 20%) values, which is consistent with published experimental results showing decrease of IS by 40% and FtF by 30% for a 30% density reduction [28, 29]. By extending the control model to include the pelvis using a similar computational approach, the biomechanical simulation results are thus assumed to be generally relevant. As the study was performed using only a single patient anatomy, anatomical variability was not investigated. Additionally, the number of configurations tested was limited and biomechanical performance assessments are focused on relative comparisons of instrumentation configurations. The tested screw diameters were relatively small as compared with most popular screw diameters used in practice. Future studies should focus on the quantification of ideal screw size, which would implicate testing larger diameters combined with other trajectory, size and design parameters. Although the present study solely focused on instrumentation geometrical parameters, future studies should also evaluate patient-related parameters such as sagittal vertical alignment or the position of the upper instrumented vertebra to provide insight on clinical applicability of the results. In this study, the impact of the modeling simplifications and assumptions can be considered as minor and do not influence the conclusions, because the focus was on the relative values between different fixation constructs.

Conclusion

Fixation achieved via transarticular sacroiliac (S1AI and S2AI) screws demonstrated higher FtF and better trabecular bone stress distribution as compared to sacral (TS1 and S1A) screw fixation, thus indicating that it can provide stronger purchase for long spine fusion surgical procedures. Biomechanical differences in failure pattern and anchorage can be explained by the improved transarticular purchase of the sacroiliac trajectory, which permits screw engagement with more cortical layers. These results suggest that, in addition to providing fewer complications and less prominent instrumentation than iliac screws, sacroiliac screws may also provide biomechanically advantageous fixation performance relative to sacral screws. Reduced fixation performance in simulated lower bone density suggests that a preoperative bone quality assessment could be a good safety indicator for intraoperative risks of failure. Higher screw diameter and cortical purchase resulted in better anchorage strength, which could increase success rates for osteoporotic patients who may have inferior bone quality. The developed model is a relevant tool to assess biomechanical fixation and could be further used and complemented by clinical and cadaveric studies to test other configurations and improve surgical planning of caudal fixation for long spine fusion.

Key points

- This finite element study allowed evaluation of fixation performance for several long instrumentation caudal anchorage strategies under pullout and toggle loading scenarios.
- A model of L5 vertebra was tested under similar loading conditions for validation purposes.
- Screws traversing more cortical layers and with higher diameters resulted in a higher force to failure under all tested loadings.
- The failure pattern depended on the screw trajectory and the load, and was generally located at the screw tip, or close to cortical–trabecular interface.

Funding Funding was provided by Natural Sciences and Engineering Research Council of Canada (Grant Number: PCIPJ-346145-16) and Aix-Marseille Université (Grant Number: ANR 11-IDEX-0001-02).

Compliance with ethical standards

Conflict of interest Funded by the Natural Sciences and Engineering Research Council of Canada (Industrial Research Chair with Medtronic of Canada, PCIPJ-346145-16), and by a research grant from Medtronic. Relevant financial activities of authors outside the submitted work: consultancy with Medtronic, grants or research support from Medtronic. The initial model used in this study also was supported in part by a grant from the A*MIDEX Foundation (Aix-Marseille University Initiative of Excellence, no ANR 11-IDEX-0001-02). The devices are FDA cleared or approved by corresponding national agency for this indication.

IRB/ethics approval All procedures performed in this study involving human participants were in accordance with the ethical standards of the institutional ethical research committee and with the 1964 Helsinki Declaration and its later amendments or comparable ethical standards. Ethical approbation for the current study was obtained from our institutional ethics review board.

References

1. Santos ER, Rosner MK, Perra JH et al (2007) Spinopelvic fixation in deformity: a review. Neurosurg Clin N Am 18:373–384
2. Ngu BB, Belkoff SM, Gelb DE et al (2006) A biomechanical comparison of sacral pedicle screw salvage techniques. Spine 31:E166–E168
3. Kuklo TR, Bridwell KH, Lewis SJ et al (2001) Minimum 2-year analysis of sacropelvic fixation and L5–S1 fusion using S1 and iliac screws. Spine 26:1976–1983
4. Wang Z, Boubez G, Shedid D et al (2018) Is S1 Alar Iliac screw a feasible option for lumbosacral fixation?: a technical note. Asian Spine J 12:749–753
5. Ebraheim N, Sabry FF, Nadim Y et al (2000) Internal architecture of the sacrum in the elderly: an anatomic and radiographic study. Spine 25:292–297
6. Zindrick MR, Wiltse LL, Widell EH et al (1986) A biomechanical study of intrapeduncular screw fixation in the lumbosacral spine. Clin Orthop 203:229
7. O'Brien JR, Yu W, Kaufman BE et al (2013) Biomechanical evaluation of S2 alar-iliac screws: effect of length and quad-cortical purchase as compared with iliac fixation. Spine 38:E1250–E1255
8. Elder BD, Ishida W, Lo SL et al (2017) Use of S2-alar-iliac screws associated with less complications than iliac screws in adult lumbosacropelvic fixation. Spine 42:E142–E149
9. Ilyas H, Place H, Puryear A (2015) A comparison of early clinical and radiographic complications of iliac screw fixation versus S2 alar iliac (s2ai) fixation in the adult and pediatric populations. J Spinal Disord Tech 28:E199–E205
10. Ishida W, Elder BD, Holmes C et al (2016) S2-alar-iliac screws are associated with lower rate of symptomatic screw prominence than iliac screws: radiographic analysis of minimal distance from screw head to skin. World Neurosurg 93:253–260
11. Bianco R-J, Arnoux P-J, Wagnac E et al (2017) Minimizing pedicle screw pullout risks: a detailed biomechanical analysis of screw design and placement. Clin Spine Surg 30:E226–E232
12. Bruna-Rosso C, Arnoux PJ, Bianco RJ et al (2016) Finite element analysis of sacroiliac joint fixation under compression loads. Int J Spine Surg 10:16
13. El-Rich M, Arnoux P-J, Wagnac E et al (2009) Finite element investigation of the loading rate effect on the spinal load-sharing changes under impact conditions. J Biomech 42:1252–1262
14. Silva MJ, Wang C, Keaveny TM et al (1994) Direct and computed tomography thickness measurements of the human, lumbar vertebral shell and endplate. Bone 15:409–414
15. Labe A (2008) Étude des mécanismes lésionnels de la région abdomino-pelvienne: applications à la traumatologie virtuelle et à la sécurité routière: Université d'Aix-Marseille II, vol. 249
16. Miller JA, Schultz AB, Andersson GB (1987) Load-displacement behavior of sacroiliac joints. J Orthop Res 5:92–101
17. Hammer N, Steinke H, Slowik V et al (2009) The sacrotuberous and the sacrospinous ligament—a virtual reconstruction. Ann Anat Anatomischer Anzeiger 191:417–425
18. Steinke H, Hammer N, Slowik V et al (2010) Novel insights into the sacroiliac joint ligaments. Spine 35:257–263
19. Garo A, Arnoux PJ, Wagnac E et al (2011) Calibration of the mechanical properties in a finite element model of a lumbar vertebra under dynamic compression up to failure. Med Biol Eng Comput 49:1371–1379
20. Wagnac E, Arnoux PJ, Garo A et al (2012) Finite element analysis of the influence of loading rate on a model of the full lumbar spine under dynamic loading conditions. Med Biol Eng Comput 50:903–915
21. Wagnac E, Arnoux PJ, Garo A et al (2011) Calibration of hyperelastic material properties of the human lumbar intervertebral disc under fast dynamic compressive loads. J Biomech Eng 133:101007
22. Riggs BL, Wahner HW, Dunn WL et al (1981) Differential changes in bone mineral density of the appendicular and axial skeleton with aging: relationship to spinal osteoporosis. J Clin Investig 67:328–335
23. Keller TS (1994) Predicting the compressive mechanical behavior of bone. J Biomech 27:1159–1168
24. Dalstra M, Huiskes R, Odgaard A et al (1993) Mechanical and textural properties of pelvic trabecular bone. J Biomech 26:523–535
25. Lotz JC, Gerhart TN, Hayes WC (1991) Mechanical properties of metaphyseal bone in the proximal femur. J Biomech 24:317–329
26. Snyder SM, Schneider E (1991) Estimation of mechanical properties of cortical bone by computed tomography. J Orthop Res 9:422–431
27. Abshire BB, McLain RF, Valdevit A et al (2001) Characteristics of pullout failure in conical and cylindrical pedicle screws after full insertion and back-out. Spine J 1:408–414
28. Burval DJ, McLain RF, Milks R et al (2007) Primary pedicle screw augmentation in osteoporotic lumbar vertebrae—biomechanical analysis of pedicle fixation strength. Spine 32:1077–1083
29. Gao MX, Lei W, Wu ZX et al (2011) Biomechanical evaluation of fixation strength of conventional and expansive pedicle screws with or without calcium based cement augmentation. Clin Biomech 26:238–244
30. Inceoglu S, Ferrara L, McLain RF (2004) Pedicle screw fixation strength: pullout versus insertional torque. Spine J 4:513–518
31. Mehta H, Santos E, Ledonio C et al (2012) Biomechanical analysis of pedicle screw thread differential design in an osteoporotic cadaver model. Clin Biomech 27:234–240
32. Santoni BG, Hynes RA, McGilvray KC et al (2009) Cortical bone trajectory for lumbar pedicle screws. Spine J 9:366–373
33. Liu CL, Chen HH, Cheng CK et al (1998) Biomechanical evaluation of a new anterior spinal implant. Clin Biomech 13:S40–S45
34. Zheng ZM, Yu BS, Chen H et al (2009) Effect of iliac screw insertion depth on the stability and strength of lumbo-iliac

fixation constructs: an anatomical and biomechanical study. Spine 34:E565–E572
35. Zheng ZM, Zhang KB, Zhang JF et al (2009) The effect of screw length and bone cement augmentation on the fixation strength of iliac screws: a biomechanical study. J Spinal Disord Tech 22:545–550
36. F543-07 AS (2009) Standard specification and test methods for metallic medical bone screws. ASTM International, West Conshohocken
37. Mattei TA, Fassett DR (2013) Combined S-1 and S-2 sacral alar-iliac screws as a salvage technique for pelvic fixation after pseudarthrosis and lumbosacropelvic instability: combined S-1 and S-2 sacral alar-iliac screws as a salvage technique for pelvic fixation after pseudarthrosis and lumbosacropelvic instability: technical note. J Neurosurg Spine 19:321–330
38. Defino HL, Vendrame JR (2001) Role of cortical and cancellous bone of the vertebral pedicle in implant fixation. Eur Spine J 10:325–333
39. Hirano T, Hasegawa K, Takahashi HE et al (1997) Structural characteristics of the pedicle and its role in screw stability. Spine 22:2504–2509 **(discussion 10)**
40. Wirth AJ, Muller R, van Lenthe GH (2012) The discrete nature of trabecular bone microarchitecture affects implant stability. J Biomech 45:1060–1067
41. Defino HL, Rosa RC, Silva P et al (2009) The effect of repetitive pilot-hole use on the insertion torque and pullout strength of vertebral system screws. Spine 34:871–876
42. Paik H, Dmitriev AE, Lehman RA Jr et al (2012) The biomechanical effect of pedicle screw hubbing on pullout resistance in the thoracic spine. Spine J 12:417–424